Intense Precipitation Events Associated with Landfalling Tropical Cyclones in Response to a Warmer Climate and Increased CO_2

ENRICO SCOCCIMARRO AND SILVIO GUALDI

Istituto Nazionale di Geofisica e Vulcanologia, and Centro Euro-Mediterraneo sui Cambiamenti Climatici, Bologna, Italy

GABRIELE VILLARINI

IIHR-Hydroscience & Engineering, The University of Iowa, Iowa City, Iowa

GABRIEL A. VECCHI AND MING ZHAO

NOAA/Geophysical Fluid Dynamics Laboratory, Princeton, New Jersey

KEVIN WALSH

School of Earth Sciences, University of Melbourne, Melbourne, Australia

ANTONIO NAVARRA

Istituto Nazionale di Geofisica e Vulcanologia, and Centro Euro-Mediterraneo sui Cambiamenti Climatici, Bologna, Italy

(Manuscript received 17 January 2014, in final form 20 March 2014)

ABSTRACT

In this work the authors investigate possible changes in the intensity of rainfall events associated with tropical cyclones (TCs) under idealized forcing scenarios, including a uniformly warmer climate, with a special focus on landfalling storms. A new set of experiments designed within the U.S. Climate Variability and Predictability (CLIVAR) Hurricane Working Group allows disentangling the relative role of changes in atmospheric carbon dioxide from that played by sea surface temperature (SST) in changing the amount of precipitation associated with TCs in a warmer world. Compared to the present-day simulation, an increase in TC precipitation was found under the scenarios involving SST increases. On the other hand, in a CO_2-doubling-only scenario, the changes in TC rainfall are small and it was found that, on average, TC rainfall tends to decrease compared to the present-day climate. The results of this study highlight the contribution of landfalling TCs to the projected increase in the precipitation changes affecting the tropical coastal regions.

1. Introduction

Heavy precipitation and flooding associated with tropical cyclones (TCs) are responsible for a large number of fatalities and economic damage worldwide (e.g., Rappaport 2000; Pielke et al. 2008; Mendelsohn et al. 2012; Peduzzi et al. 2012). In part because of the societal and economic relevance of this hazard, studies have focused on the potential changes in heavy rainfall associated with TCs in a warmer climate (Gualdi et al. 2008; Knutson and Tuleya 2004; Hasegawa and Emori 2005; Knutson et al. 2013). Despite the overall agreement about the tendency of TC rainfall to increase with greenhouse warming, the uncertainty of the projected changes is large, ranging from +3% to +37% (Knutson and Tuleya 2004; Knutson et al. 2010, 2013).

Models project a well-known increase to rainfall over land, both in terms of average and extremes (e.g., Liu et al.

Corresponding author address: Enrico Scoccimarro, Centro Euro-Mediterraneo sui Cambiamenti Climatici, Viale A. Moro, 44, 40127 Bologna, Italy.
E-mail: enrico.scoccimarro@bo.ingv.it

DOI: 10.1175/JCLI-D-14-00065.1

2009; Chou et al. 2009) and a large spatial variability is associated with changes in projected rainfall amount (Trenberth 2011; Scoccimarro et al. 2013). The goal of this study is to quantify the contribution of landfalling TCs to rainfall at different latitudes, as well as its dependence on different idealized climate change scenarios.

TCs can deliver large amounts of precipitation in a relatively short time, and tropical cyclone precipitation (TCP) represents a significant portion of total summer precipitation along the tropical coastal regions (Jiang and Zipser 2010). For instance, Larson et al. (2005) found that TCP contributes up to 20% of the total precipitation over the coast of Mexico. Individual storms, however, can account for more than 90% of the summer rainfall experienced in some regions, such as Southern California (Corbosiero et al. 2009) and Australia (Dare et al. 2012), representing a significant water management challenge.

The investigation of TCP response to different idealized global warming scenarios is made possible by the availability of a set of high-resolution general circulation models (GCMs) and simulations performed following common protocols, within the U.S. Climate Variability and Predictability (CLIVAR) Hurricane Working Group (http://www.usclivar.org/working-groups/hurricane). In our analyses, we will first assess whether these GCMs are able to reproduce TC rainfall contribution to the total rainfall at the global scale, with particular emphasis on the coastal regions. After the model evaluation, we will examine the changes in TCP for three idealized experiments: doubling CO_2, increasing the global sea

TABLE 1. Tropical cyclone count: TC annual mean number and std dev of the TC annual number.

	CLIM		2C		2K		2C2K	
	Mean	STD	Mean	STD	Mean	STD	Mean	STD
OBS	93.3	6.5	—	—	—	—	—	—
CMCC	85.3	9.8	76.6	5.4	88.5	10.8	80.4	8.0
GFDL	109.1	8.0	106.0	7.0	95.3	5.1	84.7	9.7

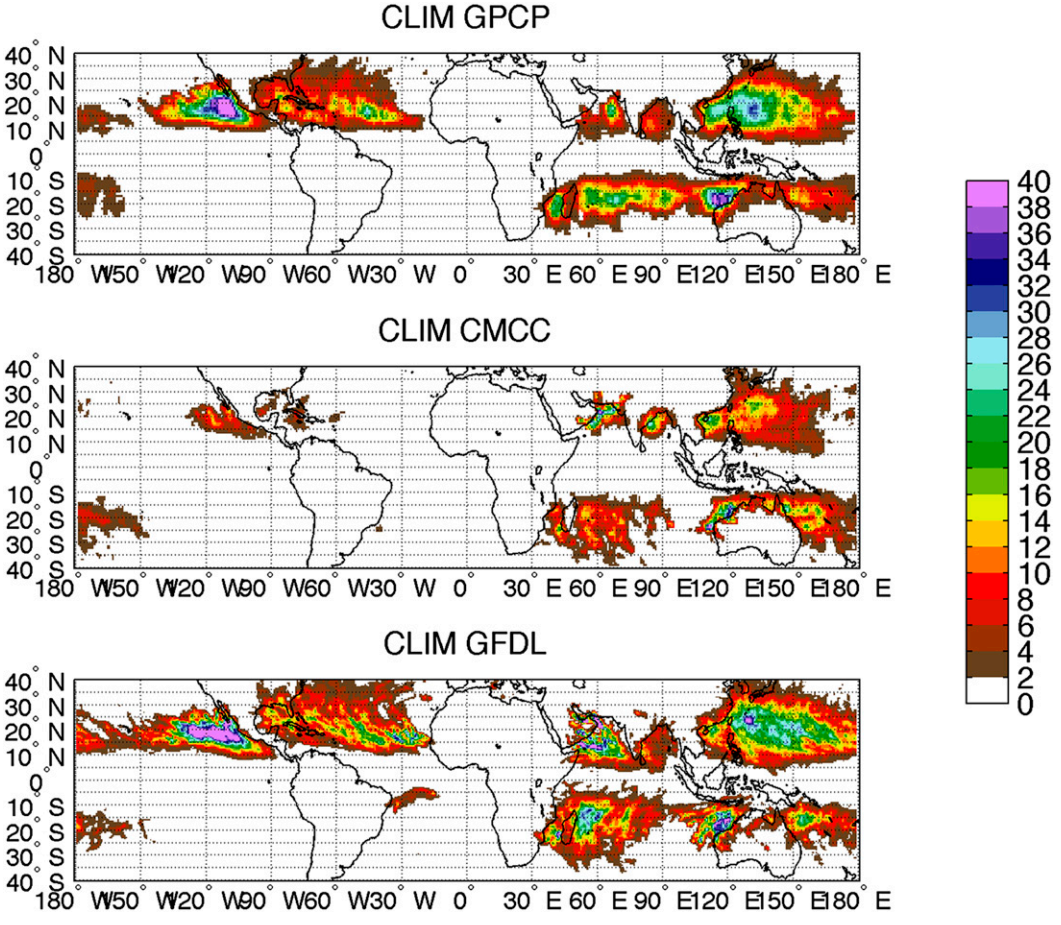

FIG. 1. Percentage of water associated with TCs in the control simulation CLIM with respect to the total annual precipitation. The accumulation is performed by taking a 6° × 6° window centered on the center of circulation. (top) Observations, (middle) CMCC, and (bottom) GFDL models. Units are in percentages.

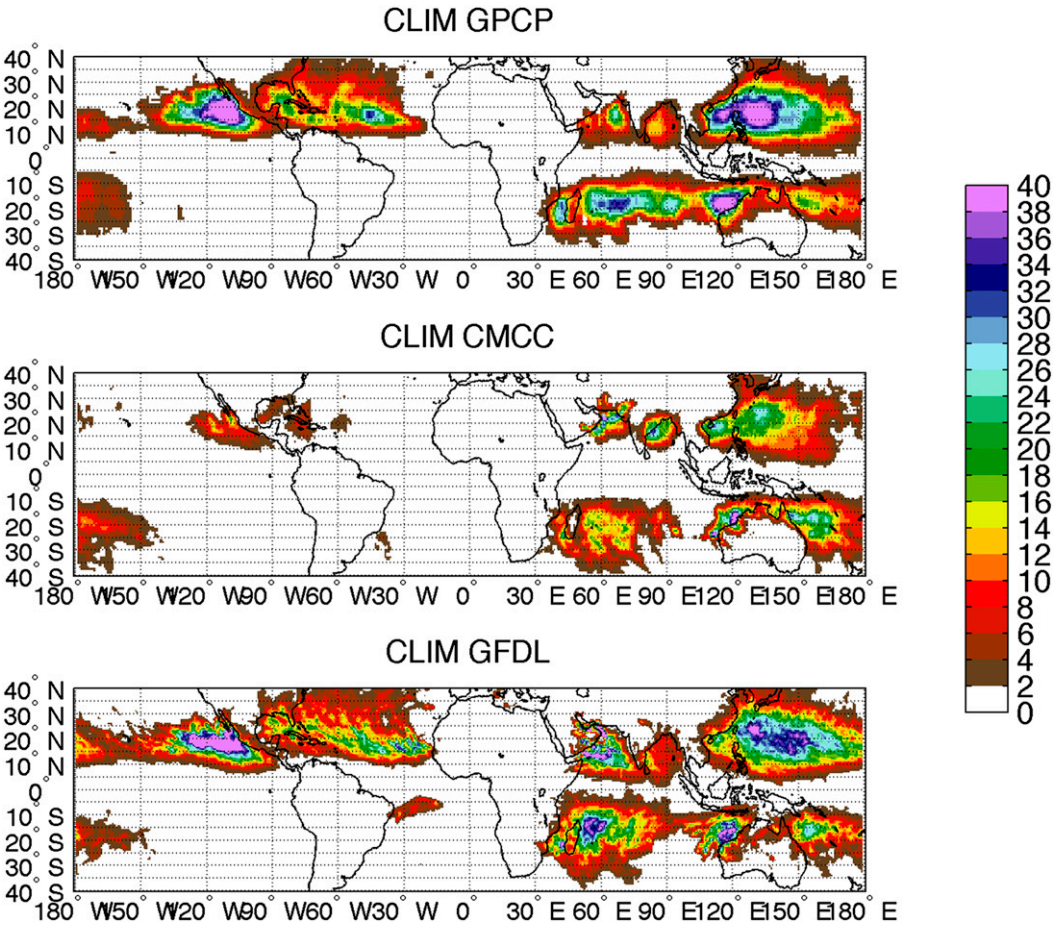

FIG. 2. As in Fig. 1, but performing the accumulation for a 10° × 10° window.

surface temperature (SST) by 2 K, and a combination of the two. These idealized experiments are not based on projected emission scenarios, but rather are designed to disentangle the role of changes in atmospheric carbon dioxide from the role played by sea surface temperatures in changing the TCs characteristics in a warmer world.

The paper is organized as follows. Section 2 describes the data, models, and simulations and provides an overview of the methodology used. Section 3 presents the results of the analyses, while section 4 summarizes the main points of the study and concludes the paper.

2. Data and methodology

a. Reference data

The reference data used in this study are TC tracks and precipitation. For the former, we use TC observational datasets available as 6-hourly data from the National Hurricane Center (NHC) and the U.S. Joint Typhoon Warning Center (JTWC). These datasets include the location of the center of circulation, maximum wind, and minimum pressure for all the TCs during the period 1997–2006. Over the same period, the Global Precipitation Climatology Project (GPCP; Huffman et al. 2001; Bolvin et al. 2009) represents the reference data to quantify the amount of water associated with TCs. The GPCP dataset is obtained by combining satellite and rain gauge data to provide daily global rainfall estimates with a 1° resolution.

b. The climate models

To investigate the ability of GCMs in representing TCP and its possible changes in a warmer climate, we leverage a set of simulations performed within the U.S. CLIVAR Hurricane Working Group. Here we focus on two models, one run by the Geophysical Fluid Dynamics Laboratory (GFDL) and one by the Centro Euro-Mediterrraneo sui Cambiamenti Climatici (CMCC). The GFDL model is a newer version of the High Resolution Atmospheric Model (HiRAM) utilized in Zhao

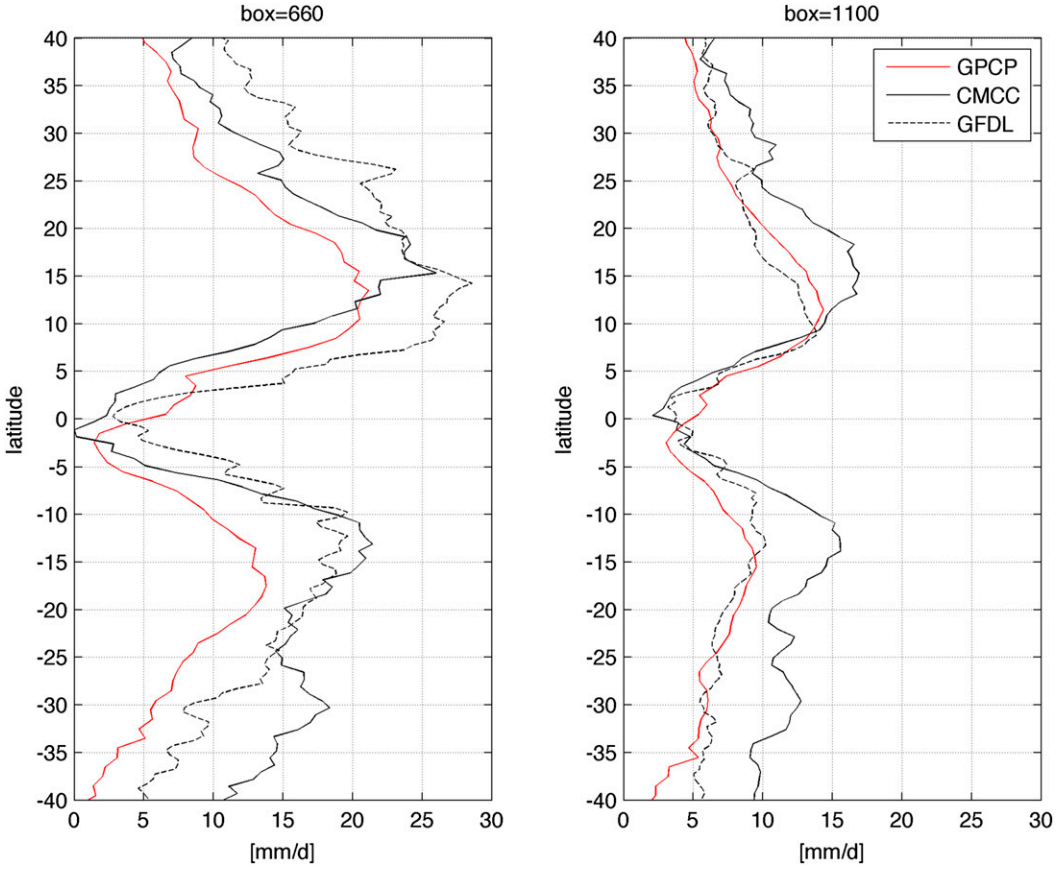

FIG. 3. TC-related precipitation amount in the CLIM experiment and observations as a function of latitude at global scale. Values are normalized by the number of TC days. Units are in mm day^{-1}.

et al. (2009, 2010), and Held and Zhao (2011) for studies of global hurricane climatology, variability, and change with global warming. The main difference is that HiRAM2.2 incorporates a new land model [GFDL land model version 3 (LM3)]. The atmospheric dynamical core of the model was also updated to improve efficiency and stability. As a result of these changes, there are minor retunings of the atmospheric parameters in the cloud and surface boundary layer parameterizations necessary to achieve the top-of-atmosphere (TOA) radiative balance. This model is also the version of HiRAM used for the GFDL participation in the Fifth Assessment Report of the Intergovernmental Panel on Climate Change (IPCC AR5) high-resolution time-slice simulations. The model uses a finite-volume dynamical core with a cubed-sphere grid topology (Putman and Lin 2007) and 32 vertical levels. The notation C180 in the model name indicates 180 × 180 grid points in each face of the cube; the size of the model grid varies from 43.5 to 61.6 km. The model uses a modified version of the University of Washington Shallow Convection Scheme (UWShCu) (Bretherton et al. 2004; Zhao et al. 2009). The choice of a less intrusive convection scheme is motivated by a desire to allow the large-scale resolved-scale convection to do much of the work.

The CMCC model is ECHAM5 (Roeckner et al. 2003) implemented with a T159 horizontal resolution, corresponding to a Gaussian grid of about 0.758° × 0.758° with 31 hybrid sigma-pressure levels with top at 10 hPa. The parameterization of convection is based on the mass flux concept (Tiedtke 1989), modified following Nordeng (1994). Moist processes are treated using a mass-conserving algorithm for the transport (Lin and Rood 1996) of the different water species and potential chemical tracers. The transport is resolved on the Gaussian grid. A more detailed description of the ECHAM5 atmospheric model performance can be found in Roeckner et al. (2006).

Rather than running the same TC tracking algorithm on both the GFDL and CMCC models, we used the tracks provided by each modeling group (Shaevitz et al. 2014, manuscript submitted to *J. Climate*). The TC tracking algorithm for the CMCC model is based on Walsh (1997) and Walsh et al. (2007) and the tracking

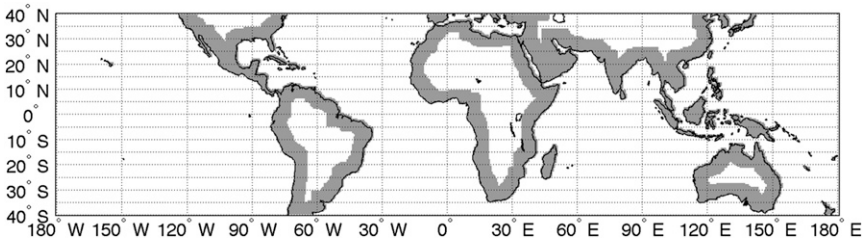

FIG. 4. Coastal regions mask. Precipitation over land is accumulated considering the gray region only.

for the GFDL model is based on Zhao et al. (2009) and Knutson et al. (2007). Detailed information on the ability of climate models in representing TCs can be found in Walsh et al. (2013).

c. *The simulations*

In this study we consider a subset of the simulations available from the U.S. CLIVAR Hurricane Working Group dataset. More specifically, we use the following four experiments:

CLIM: This is a climatological run obtained by repeating the SST climatology over the period 1982–2005 [based on the Hadley Centre Sea Ice and Sea Surface Temperature dataset (HadISST); Rayner et al. 2003] for 10 years. It is used to provide a baseline to contrast with the perturbation studies. Ozone and aerosol forcings are climatological as provided by the IPCC. Also, radiative gas concentrations are defined according to the 1992 IPCC specifications and described at the web page http://data1.gfdl.noaa.gov/nomads/forms/TropicalCyclones/exper1.html.

2C: This is a doubling CO_2 experiment. It is obtained by integrating the models with climatological SST (as in CLIM) but with a doubled concentration of atmospheric CO_2 with respect to the CLIM experiment for 10 years.

2K: This experiment is obtained by integrating the models with climatological SST (as in CLIM) and adding a 2-K globally uniform SST anomaly for 10 years.

2C2K: This experiment is made by combining the 2K and 2C perturbations.

d. *Methodology*

The amount of rainfall associated with a TC, both in models and observations, is computed by considering the daily precipitation in a 10° × 10° box around the center of the storm. According to previous studies (e.g., Lonfat et al. 2004; Larson et al. 2005; Kunkel et al. 2010), a 10° × 10° window (here defined as Box1100) is more than enough to include the majority of TC-related precipitation in most of the cases. Moreover, to better represent the contribution of the most intense precipitation patterns close to the TC eye (Villarini et al. 2014), we run the analysis also considering a smaller window (6° × 6°, here defined as Box660).

3. Results

a. *Present-day performance*

The control simulation (CLIM) performed with the two models reproduces reasonably well the TC count at the global scale for the present climate, with a 9% underestimation for the CMCC model and a 16% overestimation for the GFDL model, compared to the reference value of 93.3 TCs per year obtained from the observation for the period 1997–2006 (Table 1). The CMCC model also tends to significantly underestimate the TC count in the Atlantic basin (not shown) as confirmed by similar analyses using the coupled version of the ECHAM5 atmospheric model (Scoccimarro et al. 2011). The simulated interannual variability is slightly overestimated by both models (Table 1).

In terms of annual precipitation, both models show a positive bias over the tropical belt (not shown), especially over the intertropical convergence zone (ITCZ) and the South Pacific convergence zone (SPCZ). The difficulty in reproducing the observed precipitation patterns over these areas is a well-known problem common to many atmospheric models and is likely related to a still unsatisfactory representation of convection and planetary boundary layer processes (Dai 2006), although remote processes may also contribute (e.g., Hwang and Frierson 2013).

In this work, we aim to assess the models' ability in simulating precipitation associated with TCs and quantifying their relative changes for the three different idealized global forcing scenarios. To examine the TCP contribution to total precipitation, we accumulated TCP over the 10-yr period representing the present climate

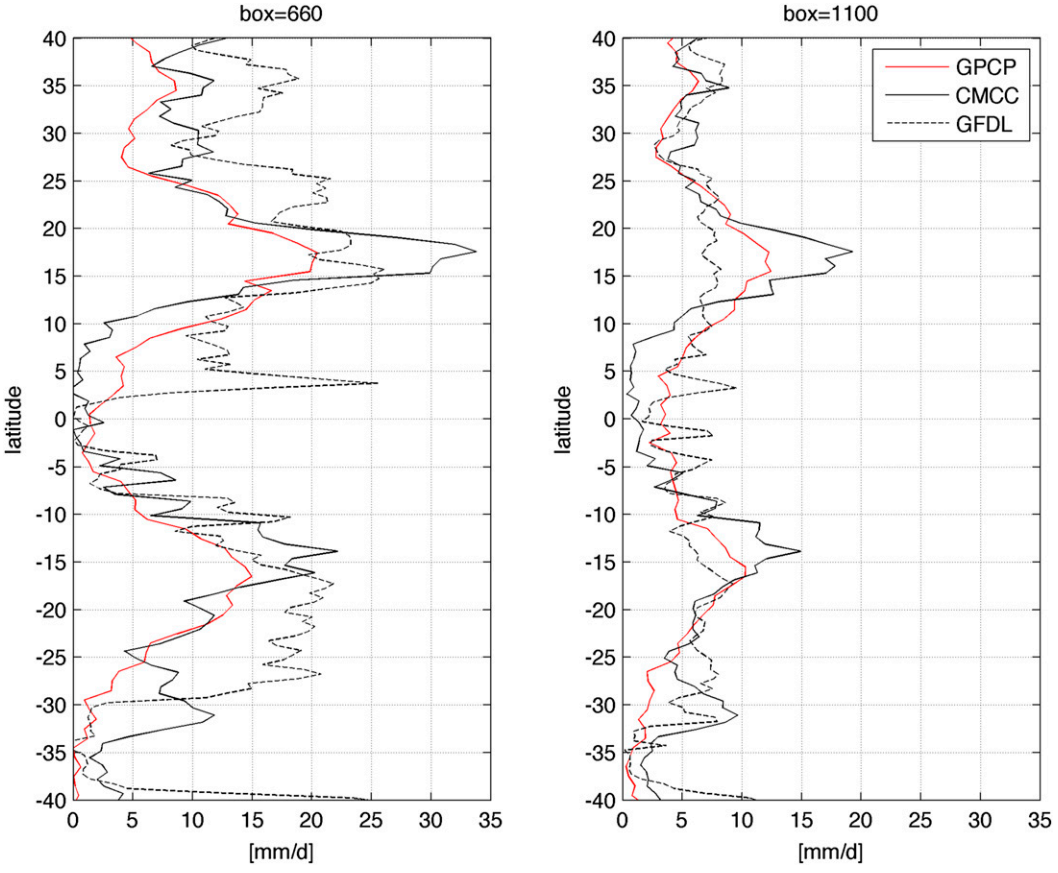

FIG. 5. TC-related precipitation amount in the CLIM experiment and observations as a function of latitude computed over considered land regions as defined in Fig. 4. Values are normalized by the number of TC days. Units are in mm day^{-1}.

and we compared it to the total precipitation for the same period. Figures 1 and 2 show the results for the observations (top) and models (middle and bottom), using the Box660 and Box1100 windows, respectively. In the observations the TC rainfall represents a large contribution to the total rainfall over the northwest Pacific, the northeast Pacific, and the northwestern part of the Australian basin. Over these regions, the amount of precipitation contribution due to TCs is as large as about 40%, reaching a maximum of 50% in the northwest Pacific. These features are captured by the simulations, despite the tendency of the CMCC model to underestimate the TCP fraction, which is presumably due, at least in part, to the ECHAM5 model deficiency in representing TCs intensity at the global scale and to the lack of TC activity over the Atlantic region (Scoccimarro et al. 2011). Notably, when the dimension of the accumulating window (Box1100 in Fig. 2 compared to Box660 in Fig. 1) is increased, the amount of TCP fraction increases, especially over the regions with high TC rainfall contributions, suggesting that resorting to a 10° × 10° box does not lead to the inclusion of non-TC-related rainfall; rather, it seems to provide a representation of TCP fraction consistent with Kunkel et al. (2010). Noteworthy, the CMCC model exhibits an excess of TCP in the Bay of Bengal, which might at least in part explain the positive model bias in the mean precipitation over this region (not shown). In terms of absolute values, the modeled TCP zonal average, normalized by TC days (hereafter TCPn) shows maximum values at about 15° in both hemispheres (Fig. 3). Both CMCC and GFDL models are able to represent the basic aspects of the latitudinal distribution of TCPn, with the GFDL model showing a better agreement to the observations, in particular in the Box1100 case (Fig. 3, right). Also, focusing on coastal regions (Fig. 4), the Box1100 TCPn tends to follow more closely the observational results compared to Box660 (Fig. 5). In the Box1100 case, the model biases are less pronounced, with a positive value of about 6 mm day^{-1} south of 25°S in both models and a meridional variability more (less) pronounced for the CMCC (GFDL) model.

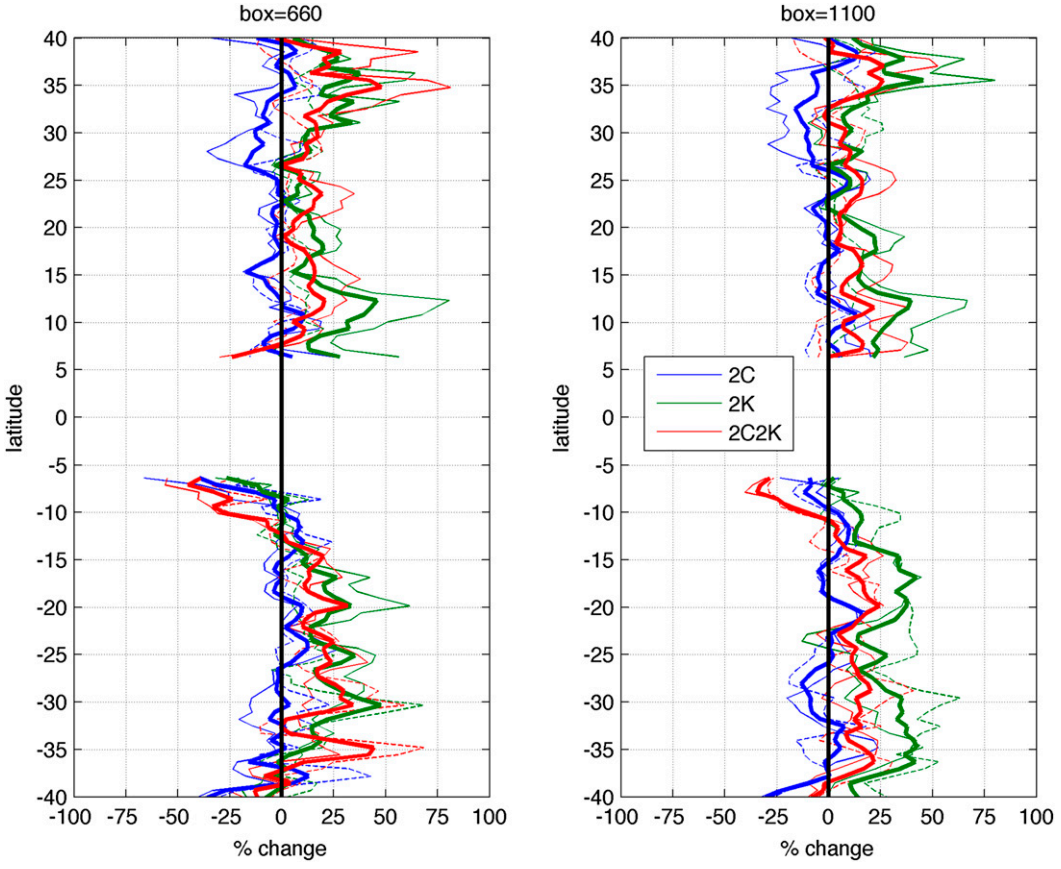

FIG. 6. Changes in TC-related precipitation amount in the 2C (blue), 2K (green), and 2C2K (red) experiments as a function of latitude. Results are shown with respect to the CLIM experiment. Solid thin lines represent CMCC results. Dashed thin lines represent GFDL results. The solid thick lines represent the average of the two models. Units are in %.

b. *Impact of idealized forcing*

In this section we show the results obtained in the 2C, 2K, and 2C2K experiments and contrast them to the control simulation (CLIM). Even though the CLIM results using the Box1100 window seem to more closely reproduce the total precipitation associated with TCs in the observations, we computed changes in TCPn using both windows (Box660 and Box1100, left and right panels, respectively, in Figs. 6 and 7). Performing the analyses on both boxes allows for assessment of the changes associated with the most intense precipitation occurring close to the TC eye (i.e., the results obtained with the Box660 window).

Changes in TCPn are very similar for the two models and show a global increase in the 2K and 2C2K experiments but not for the 2C one. The meridional distribution of TCPn changes (Fig. 6) in the 2C case shows negative values over most of the latitudes. On the other hand, the 2K and 2C2K experiments show positive changes up to 45% when considering the average of the two models (Fig. 6, red and green bold lines). The positive increase is more pronounced in the 2K experiment if compared to the 2C2K one. These results are consistent with Villarini et al. (2014), who found a widespread decrease in rainfall for the most intense TCs for the 2C experiment and a general increase in rainfall when SST was increased by 2 K. This statement holds regardless of the distance from the center of circulation and for all the ocean basins.

Focusing on the coastal region (shaded area in Fig. 4), the TCPn increase in 2K and 2C2K is even more pronounced (Fig. 7), up to 200%. In these areas even the 2C experiment shows positive changes in most latitudes. Interestingly the TCPn increase over the coastal regions (Fig. 7) is less marked at latitudes already exposed to large amount of TCPn (i.e., between 10° and 15° in the Northern Hemisphere and between 10° and 20° in the Southern Hemisphere; see Fig. 5) and more evident northward and equatorward of these belts,

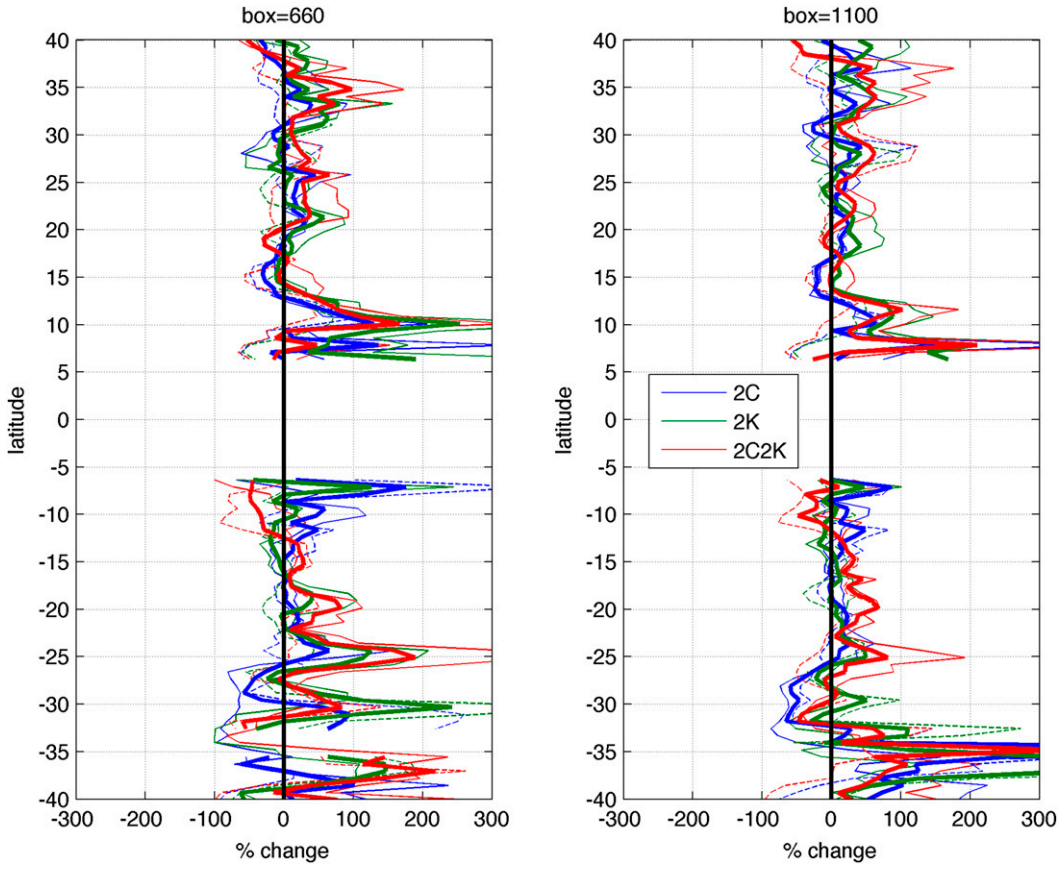

FIG. 7. As in Fig. 6, but for the land regions defined in Fig. 4.

leading to a more uniform distribution of TCPn with latitude in a warmer climate.

4. Discussion and conclusions

It is well known that atmospheric moisture content tends to increase at a rate roughly governed by the Clausius–Clapeyron equation, while the energy available to drive convection (such as the ability of the troposphere to radiate away latent heat) increases more slowly (e.g., Knutson and Manabe 1995; Allen and Ingram 2002; Held and Soden 2006; Meehl et al. 2007). Therefore, in a warmer climate we expect an increase in the water amount associated with phenomena leading to intense precipitation (such as TCs) larger than what is expected in moderate events (Scoccimarro et al. 2013). Other studies (e.g., Hill and Lackmann 2009; Wu et al. 2012) suggest that larger environmental relative humidity leads to the establishment of wider TCs (associated with larger storms), and thus more available precipitable water. In addition, Matyas and Cartaya (2009) determined that the TC precipitation distribution is influenced by the degree of outer rainband activity, which, in turn, is related to environmental specific humidity.

Our results show that the TCP is increased in the experiments with a 2-K SST increase. On the other hand, in the simulation with doubling of atmospheric CO_2, the changes in TC rainfall are small and we found that, on average, the simulated TC rainfall tends to decrease compared to the present-day climate (Fig. 6). Since environmental humidity was found to correlate with a larger hurricane rain field (Matyas 2010), and because we should expect a strong relationship between changes in available precipitable water and changes in TCP, we investigated changes in the vertically integrated atmospheric water content (WCONT) under the different idealized warming scenarios (Fig. 8). All the considered experiments show an increase in the water content over the tropical belt. The percentage increase is almost uniform across latitudes (Fig. 8, right panel; Table 2), leading to a more pronounced absolute increase over the warmer (equatorial) regions, where the WCONT shows its maxima in the CLIM experiment (not shown). The WCONT percentage increase is about 1% in 2C

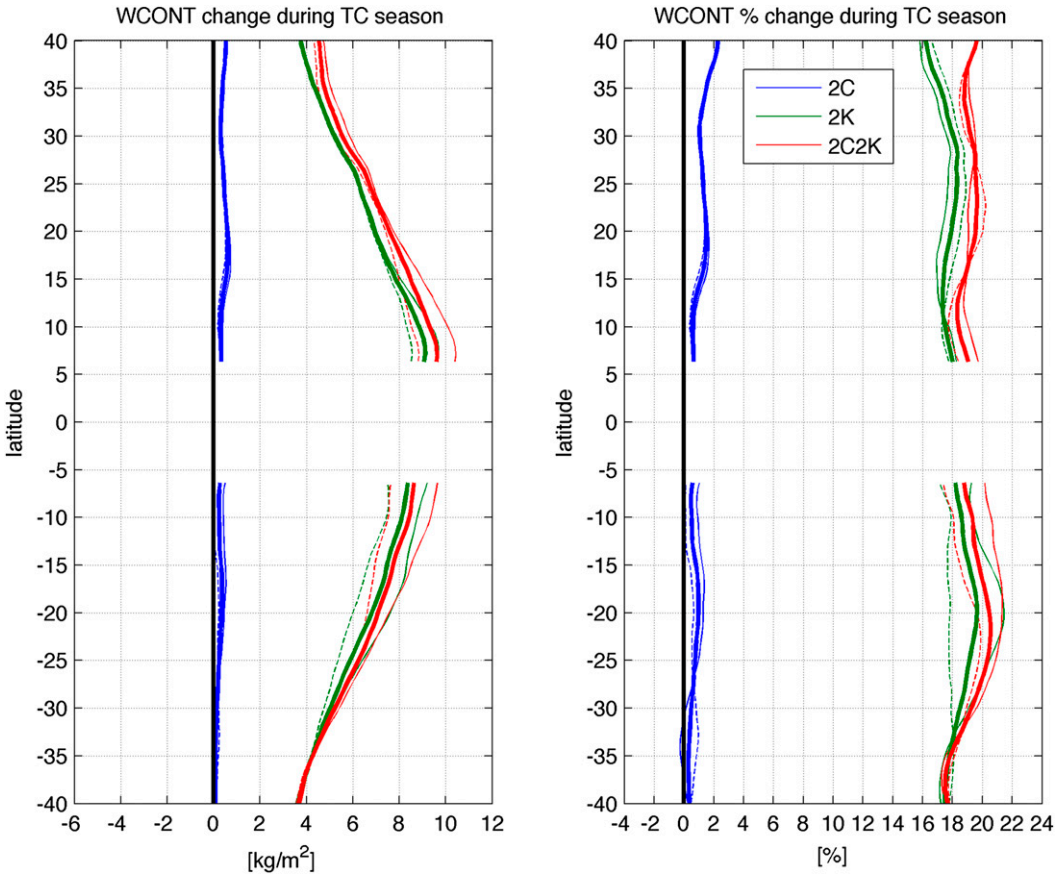

FIG. 8. Changes in vertically integrated water content (WCONT) in 2C (blue), 2K (green), and 2C2K (red) experiments as a function of latitude with respect to the CLIM experiment. Solid thin lines represent CMCC results. Dashed thin lines represent GFDL results. Solid thick lines represent averaged values. Northern Hemisphere values are computed over June–November and Southern Hemisphere values are computed over December–May. Units are (left panel) in kg m^{-2} and (right panel) in percentages.

(statistically significant at the 95% level according to a t test, over most of the latitudes, especially in the Northern Hemisphere; not shown), 18% in 2K, and 19% in 2C2K, suggesting that the 1% increment between 2K and 2C2K is mainly due to the higher atmospheric capability to hold moisture induced by the doubling of CO_2, as shown in the 2C experiment: in this experiment the globally averaged surface temperature increases of about 0.1 K, due to the warming over land. The described WCONT increases follow the Clausius–Clapeyron (CC) relation since climate models obey CC scaling fairly closely (Held and Soden 2006). According to the CC, the lower-tropospheric temperature change found in the different experiments (about 0.1 K in the 2C, 2.2 K in the 2K, and 2.4 K in the 2C2K) should lead to a WCONT increase of about 1%, 18%, and 19%, respectively, which is fully consistent with what is obtained from the models.

TABLE 2. Water balance at the global scale.

		CLIM value	2C % change	2K % change	2C2K % change
Precipitation	CMCC	2.9 (mm day^{-1})	−2.3	7.3	4.8
	GFDL	3.0 (mm day^{-1})	−2.2	6.7	4.2
Evaporation	CMCC	2.9 (mm day^{-1})	−2.3	7.2	4.7
	GFDL	3.0 (mm day^{-1})	−2.2	6.7	4.2
Atmospheric water content	CMCC	26.1 (kg m^{-2})	1.3	18.6	20.1
	GFDL	24.1 (kg m^{-2})	1.0	18.2	19.0

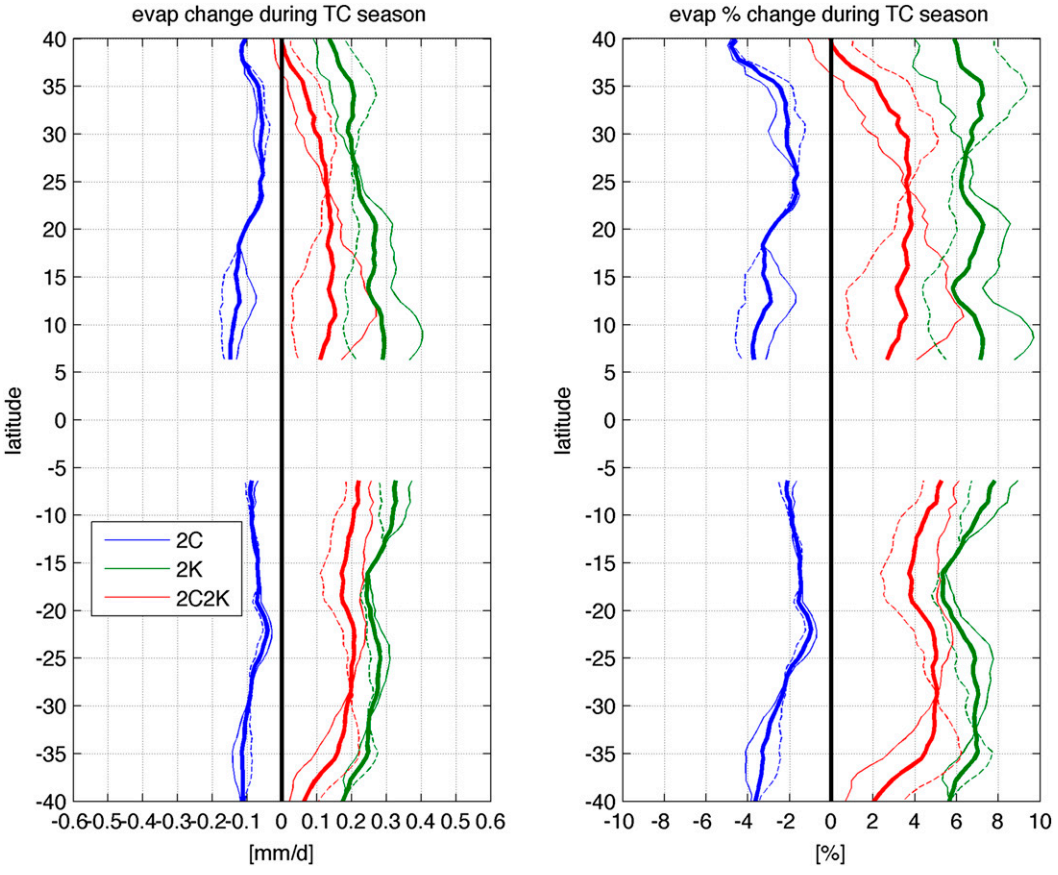

FIG. 9. As in Fig. 8, but for changes in evaporation (EVAP).

Despite the increase in WCONT in all of the three warming experiments, the doubling of CO_2 tends to reduce TCP, whereas the increase of 2 K in SST tends to increase TCP. The reason should be found in the water balance at the surface: in the 2K and 2C2K experiments (2Ks) we found a strong increase of the evaporation rate over the tropics (Fig. 9, green and red lines, respectively) due to the increase in saturated water vapor pressure at the surface. The 2-K increase in SST leads to a net increase of the evaporation rate (E). This can be easily explained considering that E is proportional to the difference between saturated water vapor at the surface (e_s) and water vapor pressure of the lower tropospheric layers (e_a), and that e_s depends on surface temperature following an exponential law, whereas e_a follows the same law, scaled by a factor (less than 1) represented by the relative humidity. Therefore, an increase in temperature has different impacts on e_s and e_a. The doubling of CO_2, on the other hand, tends to reduce E (Fig. 9, blue line; the reduction is small but statistically significant at the 95% level according to a t test, over most of the tropical domain; not shown) independently of the boundary conditions. The doubling of CO_2 in forced experiments (prescribed SST) induces a weakening effect on E, since the increase in the lower tropospheric temperature leads to an increase in e_a, associated with no changes in e_s due to the fixed temperature forcing at the surface. This effect results in an increase of the atmospheric static stability in the 2C experiment.

The CO_2 doubling tends to slow down the global hydrological cycle by about 2% (see Table 2). This is also evident in the meridional distribution of evaporation and precipitation changes (blue lines in Figs. 9 and 10, respectively) during the TC season. The 2-K SST increase induces an acceleration of the hydrological cycle on the order of 6%–7% that is reduced to 4%–5% if associated with the CO_2 doubling (Table 2; Figs. 9 and 10). The changes found in the hydrological cycle are strongly influenced by the TC precipitation: a 4% (6%) increase [as in 2C2K (2K)] in the average precipitation corresponds to an increase of about 20% (30%) in TC related precipitation.

In summary, the precipitation associated with TCs results in an increase in the experiments with a 2-K SST

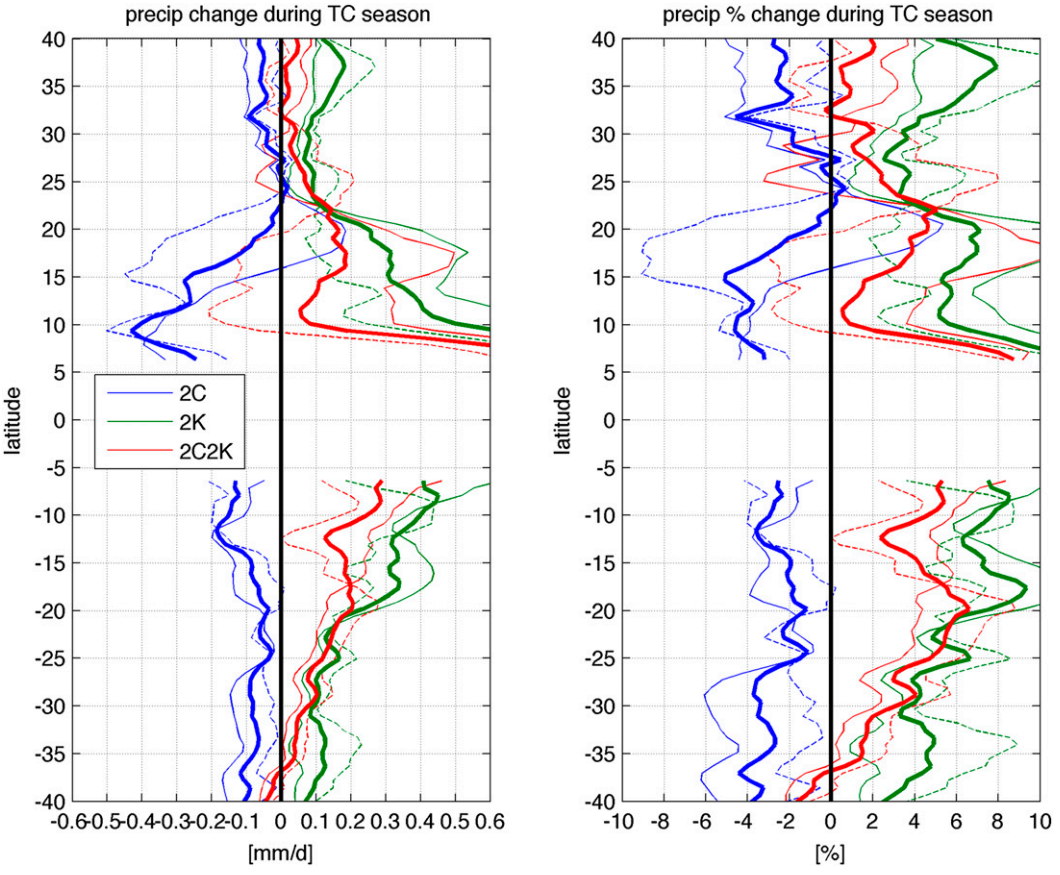

FIG. 10. As in Fig. 8, but for changes in precipitation (PRECIP).

increase and to a decrease when atmospheric CO_2 is doubled. This is consistent with the water balance at the surface, as a 2-K increase in SST leads to a net increase of the evaporation rate, while doubling the atmospheric CO_2 has the opposite effect. Moreover, TCPn (Fig. 3) tends to increase in a warmer climate (Fig. 6), leading to a more uniform latitudinal distribution of the projected precipitation associated with TCs. This is confirmed over land (Figs. 5 and 7) where the TCPn increase is projected in all of the considered warming scenarios.

Acknowledgments. This work was carried out as part of a Hurricane and Climate Working Group activity supported by the U.S. CLIVAR. We acknowledge the support provided by Naomi Henderson, who downloaded and organized the data at the Lamont data library. The research leading to these results has received funding from the Italian Ministry of Education, University and Research and the Italian Ministry of Environment, Land and Sea under the GEMINA project. Moreover this material is based in part upon work supported by the National Science Foundation under Grant AGS-1262099 (Gabriele Villarini and Gabriel A. Vecchi).

REFERENCES

Allen, M. R., and W. J. Ingram, 2002: Constraints on future changes in climate and the hydrologic cycle. *Nature,* **419,** 224–232, doi:10.1038/nature01092.

Bolvin, D. T., R. F. Adler, G. J. Huffman, E. J. Nelkin, and J. P. Poutiainen, 2009: Comparison of GPCP monthly and daily precipitation estimates with high-latitude gauge observations. *J. Appl. Meteor. Climatol.,* **48,** 1843–1857, doi:10.1175/2009JAMC2147.1.

Bretherton, C. S., J. R. McCaa, and H. Grenier, 2004: A new parameterization for shallow cumulus convection and its application to marine subtropical cloud-topped boundary layers. Part I: Description and 1D results. *Mon. Wea. Rev.,* **132,** 864–882, doi:10.1175/1520-0493(2004)132<0864:ANPFSC>2.0.CO;2.

Chou, C., J. D. Neelin, C. Chen, and J. Tu, 2009: Evaluating the ''rich-get-richer'' mechanism in tropical precipitation change under global warming. *J. Climate,* **22,** 1982–2005, doi:10.1175/2008JCLI2471.1.

Corbosiero, K. L., M. J. Dickinson, and L. F. Bosart, 2009: The contribution of eastern North Pacific tropical cyclones to the

rainfall climatology of the southwest United States. *Mon. Wea. Rev.,* **137,** 2415–2435, doi:10.1175/2009MWR2768.1.

Dai, A., 2006: Precipitation characteristics in eighteen coupled climate models. *J. Climate,* **19,** 4605–4630, doi:10.1175/JCLI3884.1.

Dare, R. A., N. E. Davidson, and J. L. McBride, 2012: Tropical cyclone contribution to rainfall over Australia. *Mon. Wea. Rev.,* **140,** 3606–3619, doi:10.1175/MWR-D-11-00340.1.

Gualdi, S., E. Scoccimarro, and A. Navarra, 2008: Changes in tropical cyclone activity due to global warming: Results from a high-resolution coupled general circulation model. *J. Climate,* **21,** 5204–5228, doi:10.1175/2008JCLI1921.1.

Hasegawa, A., and S. Emori, 2005: Tropical cyclones and associated precipitation over the western North Pacific: T106 atmospheric GCM simulation in present and doubled CO_2 climates. *SOLA,* **1,** 145–148, doi:10.2151/sola.2005-038.

Held, I. M., and B. J. Soden, 2006: Robust responses of the hydrological cycle to global warming. *J. Climate,* **19,** 5686–5699, doi:10.1175/JCLI3990.1.

——, and M. Zhao, 2011: The response of tropical cyclone statistics to an increase in CO_2 with fixed sea surface temperatures. *J. Climate,* **24,** 5353–5364, doi:10.1175/JCLI-D-11-00050.1.

Hill, K. A., and G. M. Lackmann, 2009: Influence of environmental humidity on tropical cyclone size. *Mon. Wea. Rev.,* **137,** 3294–3315, doi:10.1175/2009MWR2679.1.

Huffman, G. J., R. F. Adler, M. Morrissey, D. T. Bolvin, S. Curtis, R. Joyce, B. McGavock, and J. Susskind, 2001: Global precipitation at one-degree daily resolution from multisatellite observations. *J. Hydrometeor.,* **2,** 36–50, doi:10.1175/1525-7541(2001)002<0036:GPAODD>2.0.CO;2.

Hwang, Y.-T., and D. W. M. Frierson, 2013: Link between the double-intertropical convergence zone problem and cloud biases over the Southern Ocean. *Proc. Natl. Acad. Sci. USA,* **110,** 4935–4940, doi:10.1073/pnas.1213302110.

Jiang, H., and E. J. Zipser, 2010: Contribution of tropical cyclones to the global precipitation from eight seasons of TRMM data: Regional, seasonal, and interannual variations. *J. Climate,* **23,** 1526–1543, doi:10.1175/2009JCLI3303.1.

Knutson, T. R., and S. Manabe, 1995: Time-mean response over the tropical Pacific to increased CO_2 in a coupled ocean–atmosphere model. *J. Climate,* **8,** 2181–2199, doi:10.1175/1520-0442(1995)008<2181:TMROTT>2.0.CO;2.

——, and R. E. Tuleya, 2004: Impact of CO_2-induced warming on simulated hurricane intensity and precipitation: Sensitivity to the choice of climate model and convective parameterization. *J. Climate,* **17,** 3477–3495, doi:10.1175/1520-0442(2004)017<3477:IOCWOS>2.0.CO;2.

——, J. J. Sirutis, S. T. Garner, I. M. Held, and R. E. Tuleya, 2007: Simulation of the recent multidecadal increase of Atlantic hurricane activity using an 18-km-grid regional model. *Bull. Amer. Meteor. Soc.,* **88,** 1549–1565, doi:10.1175/BAMS-88-10-1549.

——, and Coauthors, 2010: Tropical cyclones and climate change. *Nat. Geosci.,* **3,** 157–163, doi:10.1038/ngeo779.

——, and Coauthors, 2013: Dynamical downscaling projections of twenty-first-century Atlantic hurricane activity: CMIP3 and CMIP5 model-based scenarios. *J. Climate,* **26,** 6591–6617, doi:10.1175/JCLI-D-12-00539.1.

Kunkel, K. E., D. Easterling, D. A. R. Kristovich, B. Gleason, L. Stoecker, and R. Smith, 2010: Recent increases in U.S. heavy precipitation associated with tropical cyclones. *Geophys. Res. Lett.,* **37,** L24706, doi:10.1029/2010GL045164.

Larson, J., Y. Zhou, and R. W. Higgins, 2005: Characteristics of landfalling tropical cyclones in the United States and Mexico: Climatology and interannual variability. *J. Climate,* **18,** 1247–1262, doi:10.1175/JCLI3317.1.

Lin, S. J., and R. B. Rood, 1996: Multidimensional flux form semi-Lagrangian transport. *Mon. Wea. Rev.,* **124,** 2046–2070, doi:10.1175/1520-0493(1996)124<2046:MFFSLT>2.0.CO;2.

Liu, S. C., C. Fu, C.-J. Shiu, J.-P. Chen, and F. Wu, 2009: Temperature dependence of global precipitation extremes. *Geophys. Res. Lett.,* **36,** L17702, doi:10.1029/2009GL040218.

Lonfat, M., F. D. Marks, and S. S. Chen, 2004: Precipitation distribution in tropical cyclones using the Tropical Rainfall Measuring Mission (TRMM) Microwave Imager: A global perspective. *Mon. Wea. Rev.,* **132,** 1645–1660, doi:10.1175/1520-0493(2004)132<1645:PDITCU>2.0.CO;2.

Matyas, C. J., 2010: Associations between the size of hurricane rain fields at landfall and their surrounding environments. *Meteor. Atmos. Phys.,* **106,** 135–148, doi:10.1007/s00703-009-0056-1.

——, and M. Cartaya, 2009: Comparing the rainfall patterns produced by Hurricanes Frances (2004) and Jeanne (2004) over Florida. *Southeast. Geogr.,* **49,** 132–156, doi:10.1353/sgo.0.0046.

Meehl, G. A., and Coauthors, 2007: Global climate projections. *Climate Change 2007: The Physical Science Basis,* S. Solomon and Coauthors, Eds., Cambridge University Press, 747–845.

Mendelsohn, R., K. Emanuel, S. Chonabayashi, and L. Bakkensen, 2012: The impact of climate change on global tropical cyclone damage. *Nat. Climate Change,* **2,** 205–209, doi:10.1038/nclimate1357.

Nordeng, T. E., 1994: Extended versions of the convective parameterization scheme at ECMWF and their impact on the mean and transient activity of the model in the tropics. ECMWF Research Department Tech. Memo. 206, 41 pp.

Peduzzi, P., B. Chatenou, H. Dao, A. De Bono, C. Herold, J. Kossin, F. Mouton, and O. Nordbeck, 2012: Global trends in tropical cyclone risk. *Nat. Climate Change,* **2,** 289–294, doi:10.1038/nclimate1410.

Pielke, R. A., J. Gratz, C. W. Landsea, D. Collins, M. A. Saunders, and R. Musulin, 2008: Normalized hurricane damage in the United States: 1900–2005. *Nat. Hazards Rev.,* **9,** 29–42, doi:10.1061/(ASCE)1527-6988(2008)9:1(29).

Putman, W. M., and S.-J. Lin, 2007: Finite-volume transport on various cubed-sphere grids. *J. Comput. Phys.,* **227,** 55–78, doi:10.1016/j.jcp.2007.07.022.

Rappaport, E. N., 2000: Loss of life in the United States associated with recent Atlantic tropical cyclones. *Bull. Amer. Meteor. Soc.,* **81,** 2065–2074, doi:10.1175/1520-0477(2000)081<2065:LOLITU>2.3.CO;2.

Rayner, N. A., and Coauthors, 2003: Global analyses of sea surface temperature, sea ice, and night marine air temperature since the late nineteenth century. *J. Geophys. Res.,* **108,** 4407, doi:10.1029/2002JD002670.

Roeckner, E., and Coauthors, 2003: The atmospheric general circulation model ECHAM5. Part I: Model description. MPI Rep. 349, 127 pp.

——, and Coauthors, 2006: Sensitivity of simulated climate to horizontal and vertical resolution in the ECHAM5 atmosphere model. *J. Climate,* **19,** 3771–3791, doi:10.1175/JCLI3824.1.

Scoccimarro, E., and Coauthors, 2011: Effects of tropical cyclones on ocean heat transport in a high-resolution coupled general circulation model. *J. Climate,* **24,** 4368–4384, doi:10.1175/2011JCLI4104.1.

——, S. Gualdi, A. Bellucci, M. Zampieri, and A. Navarra, 2013: Heavy precipitation events in a warmer climate: Results from

CMIP5 models. *J. Climate,* **26,** 7902–7911, doi:10.1175/JCLI-D-12-00850.1.

Tiedtke, M., 1989: A comprehensive mass flux scheme for cumulus parameterization in large-scale models. *Mon. Wea. Rev.,* **117,** 1779–1800, doi:10.1175/1520-0493(1989)117<1779:ACMFSF>2.0.CO;2.

Trenberth, K. E., 2011: Changes in precipitation with climate change. *Climate Res.,* **47,** 123–138, doi:10.3354/cr00953.

Villarini, G., D. A. Lavers, E. Scoccimarro, M. Zhao, M. F. Wehner, G. A. Vecchi, T. R. Knutson, and K. Reed, 2014: Sensitivity of tropical cyclone rainfall to idealized global-scale forcings. *J. Climate,* doi:10.1175/JCLI-D-13-00780.1, in press.

Walsh, K. J. E., 1997: Objective detection of tropical cyclones in high-resolution analyses. *Mon. Wea. Rev.,* **125,** 1767–1779, doi:10.1175/1520-0493(1997)125<1767:ODOTCI>2.0.CO;2.

——, M. Fiorino, C. W. Landsea, and K. L. McInnes, 2007: Objectively determined resolution-dependent threshold criteria for the detection of tropical cyclones in climate models and reanalyses. *J. Climate,* **20,** 2307–2314, doi:10.1175/JCLI4074.1.

——, S. Lavender, E. Scoccimarro, and H. Murakami, 2013: Resolution dependence of tropical cyclone formation in CMIP3 and finer resolution models. *Climate Dyn.,* **40,** 585–599, doi:10.1007/s00382-012-1298-z.

Wu, L., and Coauthors, 2012: Relationship of environmental relative humidity with North Atlantic tropical cyclone intensity and intensification rate. *Geophys. Res. Lett.,* **39,** L20809, doi:10.1029/2012GL053546.

Zhao, M., I. M. Held, S.-J. Lin, and G. A. Vecchi, 2009: Simulations of global hurricane climatology, interannual variability, and response to global warming using a 50-km resolution GCM. *J. Climate,* **22,** 6653–6678, doi:10.1175/2009JCLI3049.1.

——, ——, and G. Vecchi, 2010: Retrospective forecasts of the hurricane season using a global atmospheric model assuming persistence of SST anomalies. *Mon. Wea. Rev.,* **138,** 3858–3868, doi:10.1175/2010MWR3366.1.